Multiterminal Capacitance Tensor Elements of Composite Fermions and Anomalous Capacitance Peaks at Even Denominator Fillings

J. S. Moon,[1,*] J. A. Simmons,[1] J. L. Reno,[1] and B. L. Johnson[2]
[1]*Sandia National Laboratories, Albuquerque, New Mexico 87185*
[2]*Department of Physics, Western Washington University, Bellingham, Washington 98225*
(Received 6 June 1997)

We experimentally determine the propagation direction of fractional quantum Hall effect (FQHE) edge states via the symmetry properties of the multiterminal capacitances of two dimensional electron gases. Although strong asymmetries with respect to zero magnetic field appear, no asymmetries with respect to even denominator Landau level filling factor ν are seen. This indicates that current-carrying FQHE edge states propagate in the same direction as integer QHE edge states, consistent with a composite fermion gauge effective electric field. We also observe anomalous capacitance features indicative of enhanced bulk conduction at $\nu = 1/2$, $3/2$, and $3/4$. [S0031-9007(97)04624-3]

PACS numbers: 73.40.Hm, 71.10.Pm, 73.20.Dx, 73.50.Jt

In the remarkably successful composite fermion (CF) approach [1,2] to the fractional quantum Hall effect (FQHE) [3], a Chern-Simons gauge transformation attaches an even number of flux quanta to each electron, yielding a composite particle which experiences an effective magnetic field $B_{\text{eff}} = B - 2mnh/e$, where $m = 1, 2, 3, \ldots, B$ is the total magnetic field, and n is the density of the two-dimensional electron gas (2DEG). The FQHE is then viewed as the integer quantum Hall effect (IQHE) of CFs in the presence of B_{eff}. This approach is supported by measurements of the FQHE energy gaps [4] and of Fermi surface effects at $B_{\text{eff}} = 0$ [5–7].

In the IQHE regime, transport via magnetic edge states [8] within the Büttiker-Landauer picture has provided a unified description [9] of the IQHE and other transport phenomena [10]. The one-dimensional edge channels responsible for the IQHE cannot be backscattered and, thus, are highly chiral: A reversal in the sign of B results in a reversal in their propagation direction. Early efforts [11] to generalize this single electron picture to the many-body FQHE regime did not take into account the CF picture. Later, numerical model calculations of the ground state properties of FQHE edge states were carried out by treating them as IQHE edge states of CFs [12]. A naive application of these CF edge-state models implies that the propagation direction of CF edge states will reverse when B_{eff} changes sign. Recently, however, Kirczenow and Johnson [13] and Chklovskii and Halperin [14] have argued that a *gauge effective electric field*, induced by the average motion of gauge flux quanta attached to the CFs, must be included. This results in CF edge states which all propagate in the *same* direction as electrons, irrespective of the sign of B_{eff}. Until now, however, little experimental evidence on the propagation direction of FQHE edge states has been obtained. The relevance of results on edge magnetoplasmons [15] to the propagation direction of FQHE edge states *per se* is unclear.

Recently, Chen *et al.* [16] have shown that the propagation direction of edge states in the IQHE regime can be experimentally determined via the symmetry properties with respect to B of the *capacitance tensor elements* of a multiterminal sample. In this Letter, we report multiterminal capacitance tensor measurements of a high mobility 2DEG, which by contrast is clearly in the FQHE regime. Our major results are (1) for the soft-wall potential ϕ of our sample, the current-carrying FQHE edge states on either side of $3/2$ and $1/2$ all propagate in the same direction as IQHE edge states, given by $e\nabla\phi \times B$. (2) Near $\nu = 1/2$, $3/2$, and $3/4$ ($B_{\text{eff}} \approx 0$) the average motion of CFs *in the diffusive regime* is also strongly chiral, with the sign of chirality determined by B rather than by B_{eff}. Observations (1) and (2) are both consistent with a gauge effective electric field participating in the drift motion of CFs. (3) Anomalous broad flat-topped peaks centered at filling factor $\nu = 1/2$, $3/2$, and $3/4$ are observed in the capacitance between the gate and a 2DEG contact directly connected to it only by paths through the bulk.

Characteristics of the three high-mobility GaAs/AlGaAs heterostructures investigated are listed in Table I. The sample geometry is shown schematically in the inset to Fig. 1. An ac modulation voltage $Ve^{i\omega t}$ (typically 1 mV) is applied to contact G, a semitransparent metallic surface gate composed of $\sim$300 Å of Cr, which covers the edge of the 2DEG mesa and much of the bulk. The out-of-phase current $I_k(\omega)$ (of order 10 pA) is then simultaneously measured at the three diffused metallic 2DEG contacts $k = 1, 2, 3$, using phase-sensitive current preamplifiers with impedance to ground $\leq 5\ \Omega$. The capacitance tensor elements $C_{G,k}$ are obtained directly by $I_k(\omega)/[\omega V(\omega)]$ when in-phase current is negligible at

TABLE I. Sample parameters.

Sample	$n_e(10^{11}/\text{cm}^2)$	$\mu(\text{cm}^2/\text{V s})$
EMC715 (dark)	2.6	1.1×10^6
EA65 (dark)	1.2	1.3×10^6
EA100 (dark)	1.3	1.2×10^6
EA100 (after LED)	2.1	3.0×10^6

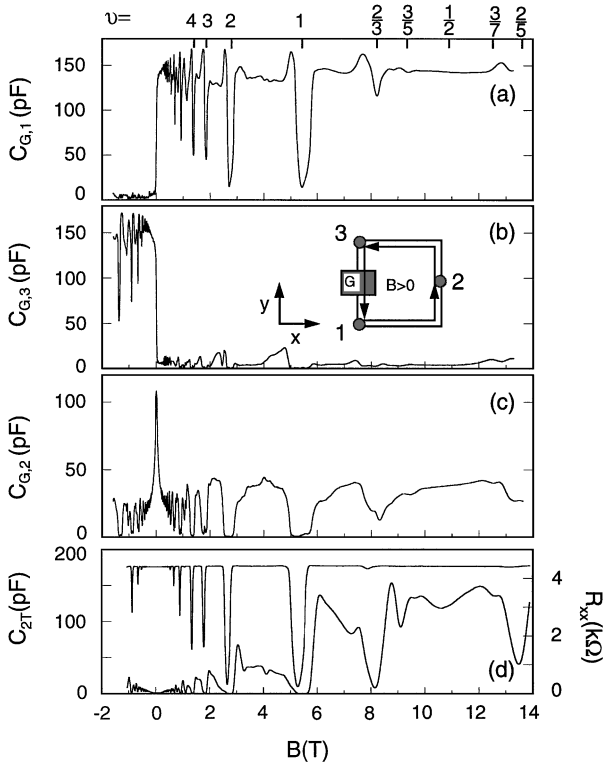

FIG. 1. Sample EA100 capacitance tensor elements for (a) $C_{G,1}$, (b) $C_{G,3}$, and (c) $C_{G,2}$. (d) Two terminal capacitance C_{2T}, and simultaneously measured ρ_{xx}. Inset shows sample geometry. Arrows indicate propagation direction of edge states for $B > 0$.

low ω (typically 200 Hz). Gate and contact dimensions and separations were typically of order 1 mm.

Figures 1(a)–1(c) show $C_{G,k}$ of sample EA100 for $T = 0.3$ K. Figure 1(d) shows both ρ_{xx} and the two terminal capacitance C_{2T}, obtained by allowing two of the 2DEG contacts to float [17]. We first discuss the IQHE regime. In contrast to the almost complete symmetry of C_{2T}, both the "edge-connected" capacitances $C_{G,1}$ and $C_{G,3}$ exhibit a striking asymmetry upon reversal of B. For positive B, $C_{G,1}$ exhibits a large background with superimposed dips associated with the formation of incompressible states in the bulk. At negative B, however, $C_{G,1}$ drops nearly to zero. $C_{G,3}$ exhibits similar behavior, only in reverse. The "bulk-connected" capacitance $C_{G,2}$, on the other hand, exhibits a large peak at $B = 0$, but falls off rapidly and symmetrically as B deviates from zero. Qualitatively similar results are obtained for the other samples.

Our results in the IQHE regime, previously observed by Chen *et al.* [16] are conceptually simplest to understand when $\nu =$ integer. In this case, the bulk is incompressible and current is carried only in the edge channels. For positive B, when the gate voltage changes, current injected from contact 3—the "edge-state sourcing contact"—remains unchanged, since it is determined only by the chemical potential in the ungated regions (see Fig. 1 inset). However, current flowing into contact 1—the "edge-state sinking contact"—*is* changed, since charge is accumulating under the gate. This results in a net current appearing at contact 1. No net current appears in contact 2 since it is directly connected to the gate only by incompressible states in the bulk. When B is negative, the roles of contacts 1 and 3 are interchanged as the edge-state propagation direction reverses. This results in the observed asymmetry in the capacitance tensor elements.

The asymmetry is also present at noninteger ν, when the bulk is compressible. Indeed, it is almost completely developed at $B \approx \pm 0.05$ T, even at high temperatures [16,18]. This indicates that the asymmetry is classical in origin, appearing when B is large enough to change the transport from an isotropically diffusive regime to one in which the Lorentz force is relevant [16]. A strong chirality occurs when the classical Hall angle θ_H (where $\tan\theta_H = \mu_{2D}B$) approaches 90°.

However, we note that even at high B, where $\theta_H \approx 90°$, a significant residual capacitance remains whenever $\sigma_{xx} \neq 0$, i.e., for noninteger ν. This cannot be explained by the simple Hall angle argument above. Rather, we present a quantitative model based on the bulk transmission probabilities between various contacts in the *ungated* region [19]. A variation in gate voltage changes the electrochemical potential μ beneath the gate, resulting in a current flow through the bulk given by $\mathbf{J} = e^{-2}\sigma\nabla\mu$, where σ is the conductivity tensor. The x and y directions are indicated in the Fig. 1 inset, with J_x representing the bulk current propagating perpendicular to the sample edge, and J_y representing the bulk current propagating parallel to the edge and, hence, eventually following the edge and reaching the edge-state sinking contact. J_x is, thus, proportional to the bulk-connected capacitance $C_{G,2}$, as well as the edge-state sourcing capacitance, $C_{G,3}$ for positive B. The total current density $\mathbf{J} = (J_x^2 + J_y^2)^{1/2}$ is proportional to the density of states beneath the gate, i.e., the two-terminal capacitance C_{2T}. Thus, $J_x \propto C_{2T}/[1 + (\rho_{xy}/\rho_{xx})^2]^{1/2}$, where we have used the expressions $\sigma_{xx} = \rho_{xx}/(\rho_{xx}^2 + \rho_{xy}^2)$ and $\sigma_{xy} = \rho_{xy}/(\rho_{xx}^2 + \rho_{xy}^2)$. The measured $C_{2T}/[1 + (\rho_{xy}/\rho_{xx})^2]^{1/2}$, shown in Fig. 2 for EA100, exhibits excellent qualitative agreement with $C_{G,2}$. Our model is

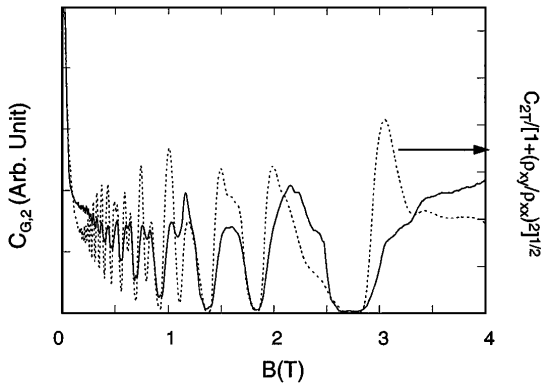

FIG. 2. Comparison of $C_{G,2}$ with measured $C_{2T}/[1 + (\rho_{xy}/\rho_{xx})^2]^{1/2}$, for sample EA100.

further supported by measurements (not shown) of $C_{G,k}$ with a dc bias on the gate, in which case the filling factor ν_G under the gate differs from that in the ungated regions ν_U. While for positive B C_{2T} shows only dips corresponding to integer ν_G, $C_{G,2}$ and $C_{G,3}$ show additional dips corresponding to $\nu_U =$ integer. These additional dips are, of course, accompanied by corresponding peaks in $C_{G,1}$ [17]. Thus, measurements of $C_{G,k}$ are strongly influenced by the bulk transport properties of the ungated regions.

We now discuss our data in the FQHE regime. By simple analogy with the capacitance asymmetries observed at $B = 0$, the question arises as to whether any such asymmetrical features appear in $C_{G,k}$ at $B_{\text{eff}} = 0$, indicating a reversal in the FQHE edge-state propagation direction. As is apparent in Fig. 1, at $\nu = 1/2$ no sudden transition nor clear signature of an asymmetry is present in $C_{G,1}$ and $C_{G,3}$. Similarly, although the presence of nearby features associated with the fractions $4/3$ and $5/3$ make the situation less clear, at $\nu = 3/2$ no definitive signature of an asymmetry is apparent. All three high-mobility samples show qualitatively similar behavior.

The absence of any distinct features asymmetric with respect to $B_{\text{eff}} = 0$ is one of our major results. It indicates that CFs in current-carrying FQHE edge states propagate in the same direction as electrons in IQHE edge states, determined by B rather than B_{eff}. This can be understood with the model of a fictitious *gauge electric field* $E_{\text{eff}} = -(J \times \hat{B})mh/e^2$ arising from the average motion of the attached flux tubes whenever there is a net CF drift current of CFs [13,14]. E_{eff} exerts a force $e\langle v\rangle \times B_{\text{eff}}$, which exactly cancels the average effective magnetic force $-e\langle v\rangle \times B_{\text{eff}}$. As a result, the *average* force seen by CFs is the same as for electrons, yielding a CF edge-state propagation direction also the same as for electrons. This picture does not contradict the results of CF geometric resonance experiments [6], since they occur in the ballistic regime where the *individual* CF magnetic force $-ev_F \times B_{\text{eff}}$ is much larger than the average force $-e\langle v\rangle \times B_{\text{eff}}$ [13,20]. As verification that the FQHE edge states are well defined (in addition to the presence of strong minima in R_{xx} at fractional ν), we also measured the gate-induced reflection of FQHE edge states in the same wafers, observing several fractionally quantized plateaus in R_{xx} in good agreement with the Landauer-Büttiker formalism [21]. In addition, our observation of anomalous capacitance peaks at even denominator ν, to be discussed below, clearly indicates the formation of CFs.

A striking feature of the CF theory is the implication that at $B_{\text{eff}} = 0$ there exists a Fermi surface with a well defined Fermi wave vector $k_F = (4\pi n)^{1/2}$. Since the measured $C_{G,k}$ depend strongly on the bulk transport properties of the ungated regions, one might expect that they would exhibit a CF Fermi surface signature near $B_{\text{eff}} = 0$. In Fig. 3(a), we show $C_{G,2}$ for sample EMC715 at 0.3 K. A distinct broad flat-topped peak, centered about $\nu = 3/2$, is apparent. The peak has a

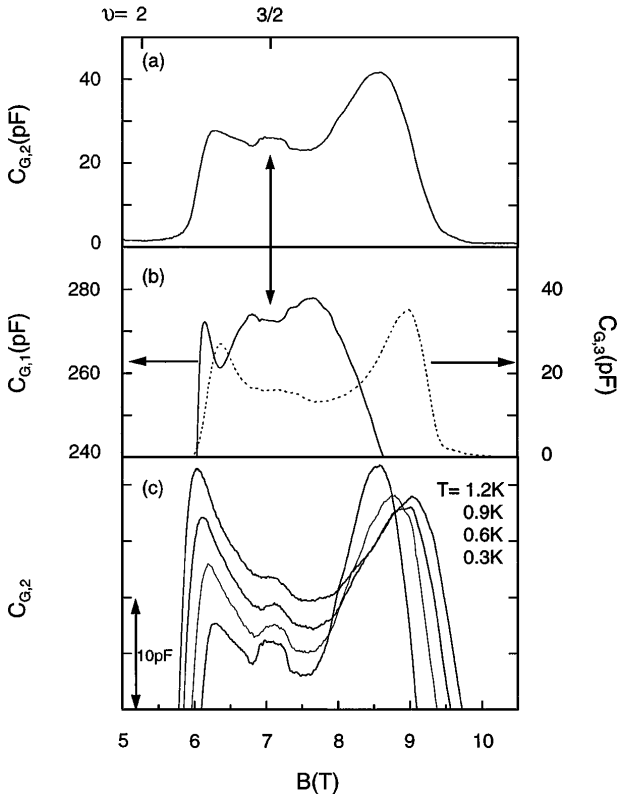

FIG. 3. Sample EMC715 capacitance tensor elements (a) $C_{G,2}$ and (b) $C_{G,1}$ and $C_{G,3}$, near $\nu = 3/2$. An anomalous capacitance peak centered at $\nu = 3/2$ appears in $C_{G,2}$. (c) Same as (a), but for several different temperatures, with curves vertically offset for clarity.

sharp turn-on at $B - B_{3/2} = \Delta B_{3/2} \approx \pm 0.26$ T, yielding a normalized half-width of $\Delta B_{3/2}/B_{3/2} \approx 0.036$. A smaller "copy" of the peak [Fig. 3(b)] is apparent in $C_{G,3}$, while an inverted peak (or broad flat-bottomed dip) is visible in $C_{G,1}$. To within experimental error, $\sum_k C_{G,k} = C_{2T}$, which is flat and featureless between $\nu = 1$ and 2. The inverted peak in $C_{G,1}$ is expected from current conservation. The presence of these features indicates an *enhancement in the bulk conductivity* near $B_{\text{eff}} = 0$. As temperature T is increased [Fig. 3(c)], the peak becomes smaller and rounded, nearly disappearing by 1.2 K. Qualitatively similar features are observed in $C_{G,2}$ for sample EA100 [Fig. 4(a)]. At 0.3 K, a broad "peak" or enhancement is seen, centered at $\nu = 1/2$ and extending from $\sim$9.8 T to $\sim$12.0 T. The normalized width of this feature is $\Delta B_{1/2}/B_{1/2} \approx 0.16$. As temperature is increased the peak diminishes, becoming nearly absent by 0.8 K. By contrast, ρ_{xx} shows no sharp features around $1/2$, exhibiting instead a gentle, temperature insensitive minimum. Figure 4(b) shows $C_{G,2}$ near $\nu = 1/2$ from sample EA65. Although fewer FQHE states are visible, the broad enhancement feature centered at $\nu = 1/2$ is again present, with a normalized width of $\Delta B_{1/2}/B_{1/2} \approx 0.16$, and remains visible at $T = 0.9$ K, even though the minimum due to the $1/3$ state is disappearing. Finally, Fig. 4(c) shows

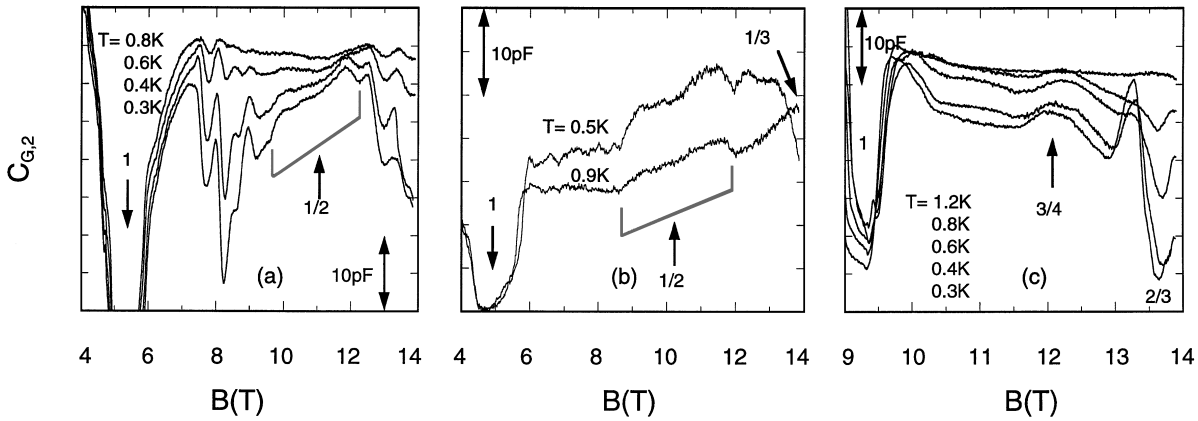

FIG. 4. Anomalous capacitance peaks, for a few different temperatures, observed (a) near $1/2$ for sample EA100, (b) near $1/2$ for sample EA65, and (c) near $3/4$ for sample EA100 after LED illumination.

$C_{G,2}$ from sample EA100 over the range $2/3 < \nu < 1$. A broad peak with a flattened top is centered at $\nu = 3/4$, and decreases rapidly with temperature, disappearing by 1.2 K.

The presence of these anomalous features at even denominator ν *cannot* be attributed to changes in the DOS of the gated 2DEG region, since in that case a peak near $1/2$ would appear for C_{2T} and for all $C_{G,k}$, contrary to what we observe. Rather, we speculate that the observed anomalous capacitance features are due to the bulk transport properties of regions *outside* the gate, which, as we have seen, strongly influence the multiterminal capacitances. In surface acoustic wave (SAW) experiments Willet *et al.* [5] have observed an enhancement in $\sigma_{xx}(q, \omega)$ at $\nu = 1/2$, when the wave vector q is (roughly) larger than both the inverse CF mean free path and the inverse CF cyclotron diameter. Although our data are at frequencies ω many orders of magnitude lower, the anomalous capacitance features show certain qualitative similarities with $\sigma_{xx}(q, \omega)$. We hypothesize that the diffusion of charge carriers in the bulk is enhanced approaching even denominator ν due to the presence of a well-defined k_F, giving rise to a peak in the bulk-connected capacitance $C_{G,2}$. Interestingly, the capacitance peak widths near $\nu = 1/2$ are similar to the widths of the CF mass divergence observed by Du *et al.* [22], $\Delta B_{1/2}/B_{1/2} \approx 0.18$, as well as to the half-widths of peaks in the CF thermoelectric power, $\Delta B_{1/2}/B_{1/2} \approx 0.14$ and $\Delta B_{3/2}/B_{3/2} \approx 0.04$, observed in Ref. [7]. Finally, we note that the capacitance features' characteristic temperature of order 1 K is similar to that predicted for the flux-binding energy of CFs [23]. Clearly, these features will provide an interesting area for future work.

We thank D. Chklovskii and D. C. Tsui for discussions and W. E. Baca for technical assistance. This work was supported by the U.S. Department of Energy under Contract No. DE-AC04-94AL85000.

*Also at Department of Physics, Michigan State University, East Lansing, MI 48824.

[1] J. K. Jain, Phys. Rev. Lett. **63**, 199 (1989).
[2] B. I. Halperin, P. A. Lee, and N. Read, Phys. Rev. B **47**, 7312 (1993).
[3] D. C. Tsui, H. L. Stormer, and A. C. Gossard, Phys. Rev. Lett. **48**, 1559 (1982).
[4] R. R. Du *et al.,* Phys. Rev. Lett. **70**, 2944 (1993).
[5] R. L. Willet *et al.,* Phys. Rev. Lett. **71**, 3846 (1993).
[6] W. Kang, H. L. Stormer, and L. N. Pfeiffer, Phys. Rev. Lett. **71**, 3850 (1993); V. J. Goldman, B. Su, and J. K. Jain, *ibid.* **72**, 2065 (1994); J. H. Smet *et al., ibid.* **77**, 2272 (1996).
[7] B. Tiecke *et al.,* Phys. Rev. Lett. **76**, 3630 (1996).
[8] B. I. Halperin, Phys. Rev. B **25**, 2185 (1982).
[9] M. Büttiker, Phys. Rev. Lett. **57**, 1761 (1986).
[10] S. Washburn *et al.,* Phys. Rev. Lett. **61**, 2801 (1988); R. J. Haug *et al., ibid.* **61**, 2797 (1988).
[11] C. W. J. Beenakker, Phys. Rev. Lett. **64**, 216 (1990); A. M. Chang, Solid State Commun. **74**, 871 (1990); A. H. MacDonald, Phys. Rev. Lett. **64**, 220 (1990).
[12] L. Brey, Phys. Rev. B **50**, 11 861 (1994).
[13] G. Kirczenow and B. L. Johnson, Phys. Rev. B **51**, 17 579 (1995).
[14] D. B. Chklovskii and B. I. Halperin, Surf. Sci. **362**, 79 (1996).
[15] R. C. Ashoori *et al.,* Phys. Rev. B **45**, 3894 (1992).
[16] W. Chen *et al.,* Phys. Rev. Lett. **73**, 146 (1994).
[17] To within experimental error, $\sum_k C_{G,k} = C_{2T}$ from the total charge conservation.
[18] At 20 K, the transition width of B increased to 0.1 T.
[19] In Ref. [16], the residual capacitance was attributed to bulk conducting regions under the gate.
[20] R. Fleischmann *et al.,* Europhys. Lett. **36**, 167 (1996).
[21] J. S. Moon *et al.,* (unpublished); A. M. Chang and J. E. Cunningham, Solid State Commun. **72**, 651 (1989).
[22] R. R. Du *et al.,* Phys. Rev. Lett. **73**, 3274 (1994).
[23] R. Morf and N. d'Ambrumenil, Phys. Rev. Lett. **74**, 5116 (1995).